Preparation of MoS_2 and WS_2 catalysts by *in situ* decomposition of ammonium thiosalts

G. Alonso [a,b], M. Del Valle [a,b], J. Cruz [b], A. Licea-Claverie [c], V. Petranovskii [a,d,*] and S. Fuentes [d,**]

[a] *Centro de Investigación Científica y de Educación Superior de Ensenada, B.C., México*
[b] *Facultad de Ciencias Químicas, UABC, Tijuana, B.C., México*
[c] *Centro de Graduados, Instituto Tecnológico de Tijuana, B.C., México*
[d] *Centro de Ciencias de la Materia Condensada, UNAM, Apdo. Postal 2681, Ensenada, B.C. 22800, México*
E-mail: vitalii@cicese.mx

Received 11 September 1997; accepted 12 March 1998

The *in situ* decomposition of ammonium thiometallates during the hydrodesulfurization (HDS) of dibenzothiophene (DBT), to obtain molybdenum disulfide and tungsten disulfide catalysts, was investigated. It was found that very efficient catalysts for the HDS of DBT were obtained by *in situ* decomposition. Mechanical uniaxial pressing of the precursors (ammonium thiometallates) affected both textural and catalytic properties of the catalysts. Surface areas of molybdenum and tungsten disulfides increased as a function of uniaxial pressing, while catalytic activities went through a maximum. For MoS_2, the hydrogenation selectivity was much higher for *in situ* catalysts than for *ex situ* ones. For WS_2 catalysts, the hydrogenation selectivity was less sensitive to the condition of decomposition (*ex situ/in situ*). The surface S/M (M = Mo, W) atomic ratio from the Auger signal decreased as a function of uniaxial pressing, while the C/M ratio remained almost constant at 1.6. The best catalyst showed an experimental S/Mo ratio that is slightly higher than the stoichiometric value. The effect of *in situ* decomposition and mechanical deformation of thiometallate precursors is discussed.

Keywords: MoS_2, WS_2, thiosalts, *in situ* activation, hydrodesulfurization, mechanochemistry

1. Introduction

Unsupported HDS catalysts are prepared by several methods, including comaceration [1], homogeneous sulfide precipitation [2] and thiosalt decomposition [3]. The last one has been widely used in preparing molybdenum and tungsten disulfide catalysts for hydrotreating processes [4]. The catalytic properties of catalysts obtained by this method are reported to depend strongly on the atmosphere, as well as heating conditions, used during the decomposition process [3]. Large variations of surface area have been observed for MoS_2 and WS_2 catalysts, from a few square meters to several hundred square meters, depending on the conditions for decomposition [5,6].

The intrinsic rates of HDS for unpromoted catalysts obtained by thiosalt decomposition are comparable to those of catalysts prepared by other methods. Cobalt-promoted unsupported catalysts prepared from decomposition of thiosalts have shown higher catalytic activities than catalysts prepared by other means [7,8].

Thiosalt decomposition is interesting as a method for designing better catalysts, since thiosalts have sulfur already bound to the metal atoms in a tetrahedral coordination, and decomposition is reported to be a topotactic reaction where the c-axis of sulfide remains the same as in the precursor [9].

A method of *in situ* decomposition of ammonium thiometallates reported by Naumann et al. [10], involving catalyst precursor salts along with sulfur-containing organic compounds in a hydrocarbon solution, pressurized with hydrogen and heated to 623 K, yielded active metal sulfides. MoS_2 catalysts with superior catalytic properties for water–gas shift and methanation were obtained by using controlled conditions during *in situ* decomposition. The cobalt- or nickel-promoted forms of the catalyst, obtained under the same conditions, were also advantageous for catalyzing hydrogenation or hydrotreating reactions [11]. Pecoraro et al. [12] have reported that catalysts prepared in this way from ammonium thiomolybdate (ATM) or ammonium thiotungstate (ATT) contained certain amounts of carbon, corresponding with the general formula $MS_{2-y}C_z$, where M = Mo or W, $0.01 \leqslant y \leqslant 0.5$ and $0.01 \leqslant z \leqslant 3.0$. The role of carbon in the design of these HDS catalysts is not fully understood.

To further the study of the *in situ* activation method, the present work reports the microstructure and textural characterization, along with catalytic activity and selectivity measurements, of *ex situ* and *in situ* prepared molybdenum and tungsten disulfide catalysts derived from ATM and ATT precursors, respectively. The effect of uniaxial pressing of precursors on the structure, composition, and catalytic properties is also investigated.

* On leave from Ioffe Physical Technical Institute, St. Petersburg, Russia.
** To whom correspondence should be addressed.

© J.C. Baltzer AG, Science Publishers

2. Experimental

2.1. Precursor preparation

The ATM and ATT crystals were synthesized according to a reported method [6]. ATM and ATT salts used as catalyst precursors were prepared in both powder and pressed forms. The powder forms of the precursors are the thiosalts without uniaxial mechanical pressing. The pressed forms were obtained by uniaxial pressing of the thiosalts to 350 or 700 MPa for 5 min in a stainless steel die. Samples were identified as ATM (or ATT)-P, ATM-350 and ATM-700, respectively. The pressed precursors were crushed in a mortar before placing them inside the reactor.

Ex situ catalysts were decomposed at 673 K, in a H_2S/H_2 15% (v/v) mix flowing at a rate of 40 ml/min during 4 h.

2.2. Standard deviation calculations

The mean standard deviations for all experimental data were calculated for three independent experiments [13] by means of the equation

$$\sigma_n = \sqrt{\frac{\sum x^2 - (\sum x)^2/n}{n}},$$

where σ is the standard deviation, x is the data, and n is the number of samples analyzed.

2.3. Catalytic activity

The HDS of DBT has been extensively studied as a model of hydrodesulfurization of petroleum feedstocks, because DBT is very difficult to desulfurize even under deep HDS conditions [14]. Most studies are performed in pressurized flow reactors. However, in some cases, batch reactors with static atmosphere may be useful to compare catalysts formed *in situ* during reaction conditions. Another advantage of batch reactors is that useful information on the selectivity for hydrogenation may also be obtained by following the composition of the reaction mixture as a function of time.

The HDS of DBT was carried out in a Parr model 4522 high-pressure batch reactor. The catalyst precursor (2.0 g), along with the dissolved reagent (5 vol% of DBT in decaline), was placed in the reactor, then pressurized to 3.1 MPa with hydrogen and heated to 623 K at a rate of 10 K/min. After the working temperature was reached, sampling for chromatographic analysis was performed during the course of each run to determine conversion versus time dependence. Reaction runs averaged about 6 h. The reaction products were analyzed using a Varian 350 gas chromatograph with a 2.0 m long, $1/8$ inch packed column containing OV-17 as separating phase.

Selectivity for a given product was calculated as the weight percentage of the product in the product mixture. There are four main products from the HDS reaction of DBT, namely, biphenyl (BIP), phenylcyclohexane (PCH), dicyclohexane (DCH) and benzene (BEN). In this case, the variation of selectivity for the main reaction products (biphenyl, phenylcyclohexane, dicyclohexane and benzene) is analyzed for MoS_2 and WS_2 catalysts subjected to changes in preparation conditions. The mean standard deviation for catalytic measurements was $\pm 3\%$.

2.4. Catalyst characterization

Characterization of catalysts was performed on samples obtained after the catalytic tests. The samples were separated from the reaction mixture by filtration, washed with isopropanol to remove residual hydrocarbons and dried under vacuum before analysis. Catalyst morphology was studied with a Jeol 5300 scanning electron microscope. Samples were set on the sample holder using graphite paint. Several fields were analyzed at different magnifications to recognize the prevalent features.

The surface composition of the catalysts was measured with a Perkin-Elmer PHI 595 scanning Auger electron spectrometer, where molybdenum MNN, tungsten NVV, sulfur LVV and carbon KLL Auger transitions, with energies of 186, 179, 152 and 272 eV, respectively, were measured. From these results, relative atomic ratios for molybdenum, tungsten, sulfur, carbon and oxygen at the surface were calculated for all samples. The mean standard deviation of the Auger peak intensities for S/M and C/M ratios were ± 3 and $\pm 6\%$, respectively.

Specific BET surface areas were determined with a Micromeritics Gemini 2060 surface area analyzer, using nitrogen adsorption at 77 K. Samples were degassed under flowing argon at 473 K for 2 h before nitrogen adsorption. The mean standard deviation for surface area measurements was $\pm 2\%$.

Differential thermal analysis (DTA) and thermogravimetric analysis (TGA) of thiosalts were made on a Stanton Redcroft DTA-TGA model STA-80, under dry nitrogen flow, from 293 to 1073 K and with a heating rate of 10 K/min. The mean standard deviation for DTA-TGA measurements was $\pm 2\,^{\circ}\mathrm{C}$ and $\pm 3\%$ (w/w).

The X-ray diffraction (XRD) measurements of the resulting *in situ* catalysts were made in a Philips X'Pert analytical diffractometer, equipped with a curved graphite monochromator, using Cu K_α radiation.

3. Results

3.1. Surface area, catalytic activity and selectivity

The surface areas of the catalysts, after *in situ* decomposition of their precursors and HDS reaction, are summarized in table 1. The surface area of MoS_2 catalysts tends to increase slightly (up to 15%) as greater mechanical pressure is applied to their precursors. In the case of WS_2, surface area increases for intermediate pressure (up to 68%), and slightly decreases for higher pressure. Molybdenum

Table 1
Specific surface areas and initial rate constants for HDS of *ex situ* and *in situ* prepared molybdenum sulfide and tungsten sulfide catalysts.

Sample	Specific surface area (m^2/g)	k (specific) 10^{-6} mol/l g s
ex situ ATM-P	5	3.4
ATM-P	74	4.5
ATM-350	80	5.1
ATM-700	85	4.4
ex situ ATT-P	49	2.7
ATT-P	47	4.0
ATT-350	79	4.6
ATT-700	73	3.2

Table 2
Products selectivity and HYD/HDS ratio of *in situ* and *ex situ* activated samples.

Sample	DCH (%)	BIP (%)	PCH (%)	BEN (%)	HYD/HDS
ex situ ATM-P	29	**55**	15	1	0.8
ATM-P	**50**	26	17	7	2.6
ATM-350	30	**37**	28	9	1.6
ATM-700	**50**	26	18	6	2.6
ex situ ATT-P	**41**	31	21	7	2.0
ATT-P	**48**	26	20	6	2.6
ATT-350	**45**	30	19	6	2.1
ATT-700	**40**	25	21	14	2.4

disulfide obtained by *ex situ* decomposition of ATM-P has a very low surface area, while the surface area of *ex situ* WS_2 catalyst is similar to the surface area of the *in situ* ATT-P catalyst.

For both MoS_2 and WS_2 catalysts, the conversion of DBT increased linearly with time, corresponding to an apparent zero-order rate law under these conditions. As a measure of catalytic activity, table 1 includes the initial rate constants calculated from the slope of these plots and assuming zero-order.

The HDS activity along the series of samples follows the same trend for the molybdenum and tungsten systems. *In situ* catalysts show higher activities than *ex situ* ones, and specific rate constants go through a maximum with the amount of applied uniaxial pressure. While surface area is increased to some extent by uniaxial pressing, it seems to have no direct relationship with the catalytic activity.

The reaction followed two main paths, one that removes the sulfur atom from DBT molecules (HDS path), and another that hydrogenates aromatic rings (HYD path), with some occasional cracking of BIP that yields BEN. Thus, the ratio of product concentrations (PCH + DCH)/(BIP) is taken as the HYD/HDS selectivity ratio.

Data of equilibrium selectivity after 6 h of reaction are listed in table 2 for all samples. Distribution of products depends strongly on applied pressure for MoS_2 catalysts, while there is no such dependence for WS_2 catalysts. For all but one of the precursors, DCH is the main product (up to 50%, see table 2), with ATM-350 yielding BIP as the main product.

For MoS_2, the *ex situ* catalysts show lower HYD/HDS ratios and lower cracking than the *in situ* catalysts. Uniaxial pressing of MoS_2 precursors to 350 MPa severely decreases the HYD/HDS ratio due to a relative increase of BIP. Higher uniaxial pressing of the precursors leads to selectivities comparable to those of the unpressed precursors. For WS_2 catalysts, the same tendency is observed, although less pronounced.

It should be noted that the ATM-350 *in situ* catalyst has both the highest catalytic activity and the lowest HYD/HDS ratio of all the catalysts tested (table 2).

3.2. X-ray diffraction

The XRD patterns of the *in situ* catalysts show several very broad and low intensity peaks. Such patterns resemble the poorly crystallized MoS_2 prepared at 673 K, discussed by Liang et al. [15]. According to the diffraction pattern in figure 1, mechanical pressing of ATM decreases the (002) peak in the resulting MoS_2 catalysts, while all other peaks remain the same. The modeling study of Liang et al. [15] produces similar patterns when it modifies the stacking of MoS_2 layers while preserving the internal crystalline order, which suggests that mechanical pressing of precursors may have the same effect. In contrast, no effect of uniaxial pressing on the diffraction pattern of WS_2 catalysts was observed, implying that the WS_2 derived from pressed precursors retains its overall crystalline order.

3.3. Scanning electron microscopy

Scanning electron microscopy (SEM) is used to observe any morphological variations in sample particles due to the applied mechanical pressing. The SEM micrograph for

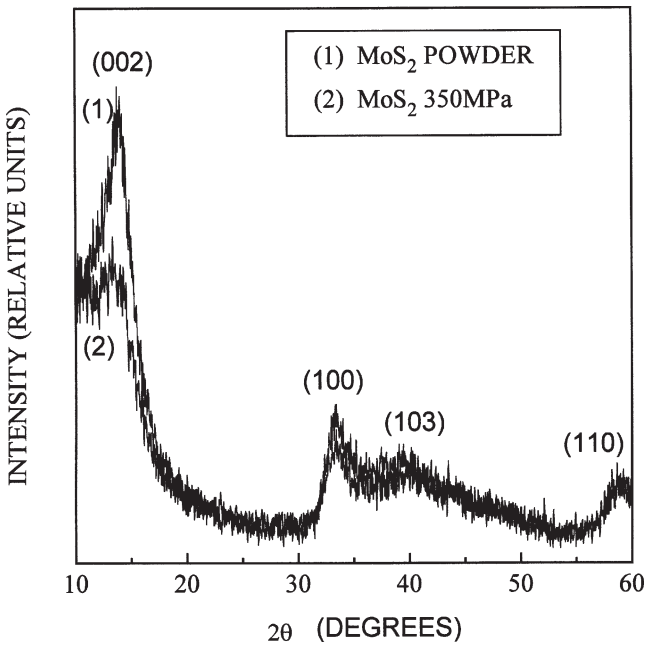

Figure 1. XRD patterns for MoS_2 catalysts prepared from (1) unpressed and (2) 350 MPa pressed precursors.

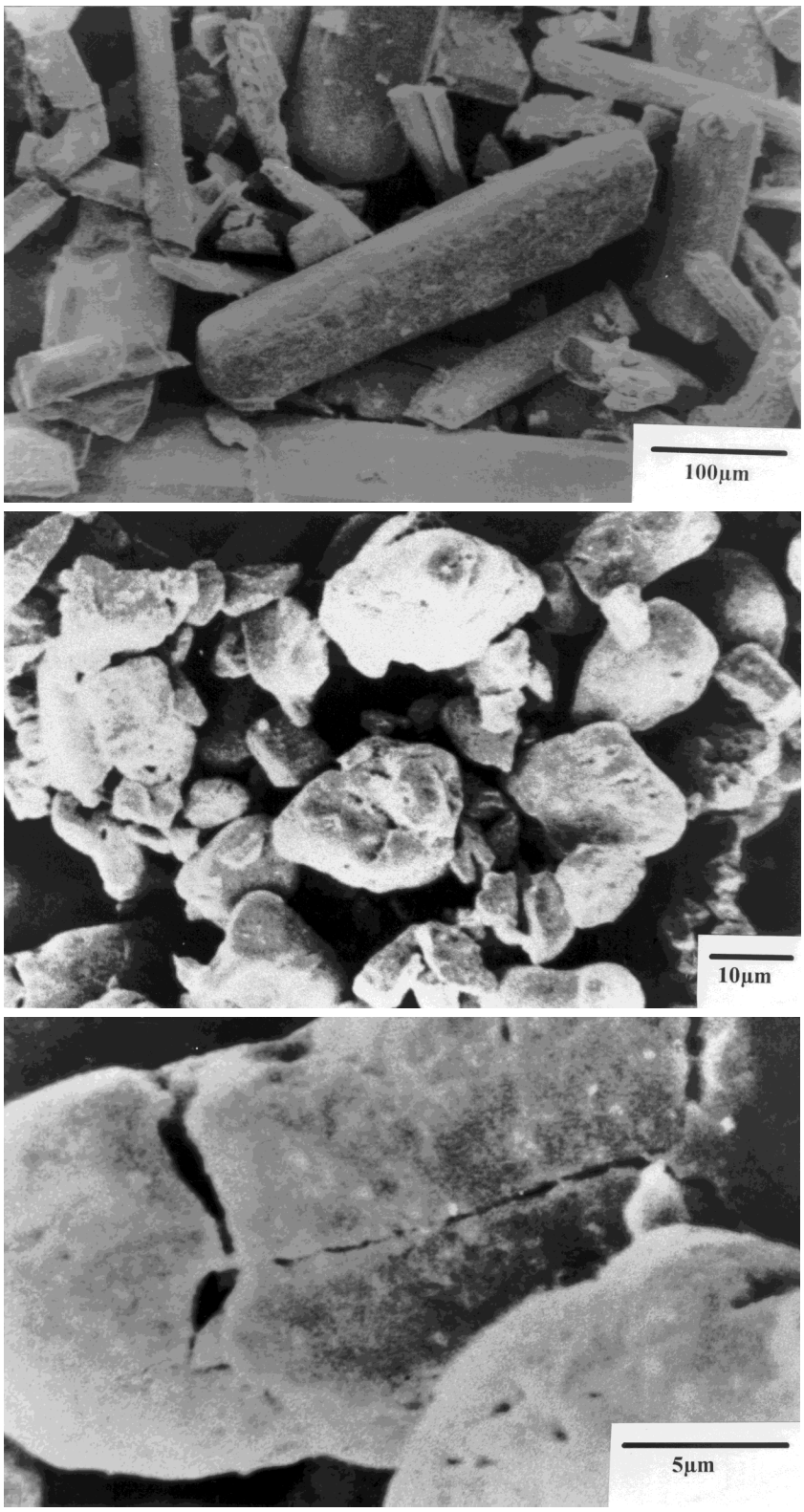

Figure 2. SEM micrograph of (a) as-synthesized ATM crystals, (b) MoS_2 catalyst particles, (c) a particle of pressed-derived catalyst ATM-350.

ATM in figure 2(a) is very similar to that of ATT. As-synthesized ATM and ATT consist of brick-shaped elongated crystals, 100–500 μm in length; the crystals break during pressing to form pellets. All the samples after the catalytic tests are composed of rounded irregular particles, with an average size of 20–30 μm, like those shown for MoS_2 in figure 2(b). No significant difference can be observed with respect to size distribution and shape of particles of the *in situ* formed MoS_2 and WS_2 catalysts. The surface of individual particles of pressed-derived catalysts

ATM-350 at higher magnification is shown in figure 2(c). As a general trend, the amount of cracks increases with pressure.

3.4. Thermal analysis

The data obtained from the DTA-TGA thermograms of different precursors are summarized in table 3. For powder ATM, thermograms show two neighboring initial steps (with temperatures T_1' and T_1) instead of the single one found in pressed samples, with a combined weight loss that is higher than expected for MoS_3 formation. Some of the peaks in the decomposition pattern of the powder ATM are slightly shifted with respect to the decomposition pattern of the pressed samples. The decomposition pattern of the powder samples also includes an early transition at 406 K, which is not found in the pressed samples. For ATT precursors, pressed samples have slightly higher temperatures of decomposition than powder ones, indicating that thermal stability has increased by pressing the precursors.

3.5. Auger electron spectroscopy (AES)

The AES analysis is carried out on samples obtained after the catalytic test to determine the surface composition of the catalysts. The atomic ratios S/M and C/M (where M = Mo or W), as a function of applied mechanical pressure, are shown in table 4. The sulfur-to-metal ratio decreases with increasing pressure from 5.0 to 3.7, while the C/M ratio remains about the same (aproximately 1.6), except for sample ATM-700. No oxygen was found on the surface of the freshly prepared samples.

Table 3
Thermogravimetric analysis of ATM and ATT precursors in nitrogen atmosphere.

	ATM-P	ATM-350	ATT-P	ATT-350
T_1' (K)	406	–	–	–
Δw_1 (exp.) (wt%)	5.0	–	–	–
T_1 (K)	423	422	448	465
T_2 (K)	491	492	535	540
Δw_1 (exp.) (wt%)	27.7	24.5	19.6	18.4
Δw_1 (theor.) (wt%)	26.2	26.2	19.6	19.6
T_3 (K)	676	670	643	651
Δw_2 (exp.) (wt%)	11.9	13.6	12.2	12.2
Δw_2 (theor.) (wt%)	12.3	12.3	9.2	9.2

Δw_1 and Δw_2 are experimental and theoretical weight losses of sample during the first step (in the temperature range between initial (T_1) and intermediate (T_2) temperatures), and the second step (in the temperature range between intermediate (T_2) and final (T_3) temperatures) of thermal decomposition, respectively.

Table 4
Relative surface composition of M (Mo or W), S and C, measured by AES of *in situ* prepared molybdenum sulfide and tungsten sulfide catalysts.

Sample	Atomic ratios (normalized to Mo or W)	
	S/M	C/M
ATM-P	5.0	1.5
ATM-350	4.7	1.5
ATM-700	3.7	2.0
ATT-P	4.5	1.7
ATT-350	4.0	1.6
ATT-700	3.7	1.7

4. Discussion

The decomposition of thiosalts has been widely investigated by thermal analysis [4,16–19]. It has been observed that the evolution from thiosalt precursors to MoS_2 (hcp), as indicated in the following sequence

$$(NH_4)_2MoS_4 \rightarrow MoS_3 \rightarrow MoS_2 \text{ (amorphous)} \rightarrow MoS_2 \text{ (crystalline)}$$

occurs in three main steps: (a) elimination of ammonium disulfide, (b) elimination of sulfur, and (c) aggregation and ordering of crystallites.

According to the literature, the first step is slightly endothermic; MoS_3 is formed releasing ammonia and hydrogen sulfide to the gas phase in the temperature range 473–573 K. The second step is notably exothermic, yielding a highly disordered – poorly crystalline – MoS_2 as it eliminates sulfur (or hydrogen sulfide, if excess hydrogen is present) between 623 and 673 K. Finally, the third step occurs at temperatures above 773 K without significant weight loss and involves a re-stacking process of the MoS_2 crystallites. The degree to which sulfur is removed and the lattice becomes organized depends on the temperature.

The process of decomposition of tungsten thiosalts has received much less attention than the corresponding molybdenum thiosalts. Earlier studies report that textural and structural properties of WS_2 catalysts, obtained by thiosalt decomposition, are very similar to that of MoS_2 [20,21]. More recently, Ramanathan et al. have shown that the morphological, chemisorptive and hydrogenation properties of WS_2 catalysts prepared by *in situ* decomposition are also comparable to those of MoS_2 [6]. Some differences, reported between MoS_2 and WS_2 catalysts, have been attributed to a larger resistance to sintering [5] and a better crystalline organization [22] of WS_2 compared to MoS_2, when treated under the same conditions.

In this work, and according to table 3, the DTA-TGA analyses of non-pressed samples in nitrogen are very similar. Appearance of the first small step (5% of weight lost) in the thermogram of ATM-P seems due to the elimination of impurities. Since ATM is crystallized from a saturated aqueous solution, some amount of water can be expected to contaminate the thiosalt. Such an early-run weight loss has already been attributed to dehydration of the starting material [23]. The pressing of ATM helps eliminate this water, so that the decomposition pattern of ATM-350 becomes nearly identical to that reported in the literature [16]. As seen in table 3, the ATM-P sample is the only thiosalt which initially decomposes to a sulfur-deficient trisulfide (MoS_{3-x}). This observation agrees with the TGA analysis

of ATM reported by Wang et al. [23]. Pressing of precursors has only a slight influence on the pattern of thermal decomposition of both ATM and ATT, and no effect on the stoichiometry of the final products, namely MoS_2 and WS_2. Since there are no large changes in the DTA-TGA pattern, no variation of the primary crystalline structure is inferred.

In the *in situ* experiments, the set temperature of the reactor (623 K) corresponds to the lower limit of the decomposition temperature for the second step (decomposition of MS_3 to $MS_2 + S$), and a sulfur-rich MS_{2+x} phase may be expected. Intermediate compounds showing S/Mo stoichiometries from 2.4 to 2.7 have been reported in the literature [24,25]. However, amorphous MoS_3 is very sensitive to the presence of hydrogen, which lowers the onset of its decomposition [16].

The S/M stoichiometry of MoS_2 and WS_2 unsupported catalysts prepared by thiosalt decomposition has been observed to vary as a function of the gas atmosphere [26,27].

The AES analysis of crystalline MoS_2 typically tends to overweigh the sulfur signal (and thus the S/M ratio), in part due to the layered structure of MS_2 where the four nearest-surface layers have an S/M ratio of three, but also because the extinction coefficients of the layers involved are different. Previous results have revealed that S/Mo ratios of 3.9–4.1 are characteristic for a MoS_2 single crystal [28], and thus the mean value of S/M = 4.0 is used as the reference value for the surface stoichiometry of MoS_2 determined by AES.

The surface S/M ratio of the *in situ* catalyst samples analyzed by AES is found to differ from the bulk S/M ratio reported by Pecoraro [12]. According to table 4, variations of the S/M ratio from 5.0 to 3.7 for MoS_2, and from 4.5 to 3.7 for WS_2 samples clearly indicate that uniaxial pressing helps eliminate sulfur from the surface, either during thiosalt decomposition or during the HDS reaction. *In situ* molybdenum and tungsten sulfide catalysts obtained from ATM-P and ATT-P have a higher S/M ratio than the reference value, suggesting that some of the sulfur generated by the reaction remains on the surface. The ratio is found to decrease for the catalysts as their precursors are subjected to greater mechanical pressure. For ATM-700 and ATT-700 the S/M ratio is smaller than the reference value, which means that the surface composition of the catalysts is deficient in sulfur. The sulfur deficiency may be attributed to variations of exposed planes at the surface, e.g., formation of border planes instead of basal ones is expected to decrease the S/M ratio.

Deformation of the ATM and ATT precursors by uniaxial pressing generates defects in the crystal structure which after decomposition increase the border surfaces on the sulfide catalysts.

Surface carbon content, as measured by AES, is nearly the same for all samples and quite uniform, averaging 1.6 monolayers of carbon. This carbon is derived either from the aromatic rings of the decaline or the HDS products during the course of the reaction.

When heated under hydrogen at temperatures as low as 498 K, the XRD patterns of ATM samples develop a broad (002) band corresponding to the poorly crystalline structure of MoS_2 [9]. The XRD results of this work confirm this observation both for ATM and ATT. With respect to uniaxial pressing, the XRD patterns show contrasting behavior between MoS_2 and WS_2 catalysts. For MoS_2, the (002) peak (c-direction) broadens and decreases in intensity for the pressed sample, indicating that layer stacking is affected. Exfoliation procedures are reported to give monolayers of MoS_2, resulting in the nearly complete disappearance of the (002) diffraction line [29]. The experimental results suggest that thinner crystallites are formed when the uniaxial pressure is applied to thiomolybdate crystallites. For WS_2 catalyst, no influence of mechanical pressure on XRD pattern is found.

The catalytic activity and the S/M ratio of MoS_2 and WS_2 catalysts for the HDS of DBT behave differently with respect to the uniaxial pressing of precursors. While specific rates go through a maximum from powder to highly pressed samples, the S/M ratios decrease steadily (tables 1 and 4). According to the experimental results, the carbon-coated catalysts with S/M ratios near stoichiometric show the highest catalytic activity. The improved performance in catalytic activity of *in situ* catalysts compared to *ex situ* ones is attributed to a better stability of the catalyst surface due to the presence of carbon, along with more efficient heat dissipation during the exothermic step of MS_3 decomposition. Further experiments are needed to elucidate the correlation between surface S and C with catalytic activity.

It should be noted that, even though the activity changes induced by uniaxial pressing are modest, they are beyond experimental error. The mean deviation calculated for three similar experiments is $\pm 2.5\%$. Contribution of internal diffusion to the rate of catalytic activity is negligible, according to calculations of the Thiele modulus [30].

Variations of the selectivity ratio HYD/HDS are observed between *ex situ* and *in situ* unpressed catalysts. The *in situ* catalysts show higher selectivity for hydrogenation products (DCH and PCH). Changes in the selectivity ratio due to pressing are also found. For both MoS_2 and WS_2 catalysts, HYD/HDS decreases when the precursor is uniaxially pressed to 350 MPa, indicating that either an increase of HDS sites or a decrease of hydrogenation sites occurs. It is probable that mechanical pressing generates more HDS by creating new edge sites, as shown by XRD for MoS_2 catalysts, since a general increase of activity is observed as the selectivity changes.

The effect of uniaxial pressing on the structure of crystals is known as mechanochemistry. Intensive mechanical forces have been shown to produce changes in the crystal structure of crystalline solids, including permanent lattice defects, polymorphous transformations, total amorphization and a definite increase of surface free energy [31]. All these are forms by which a high share of mechanical energy can be permanently stored in the catalysts precursors and thus

can contribute to create defects which are potential sites for catalytic reactions. The mechanical pressing of thiometallates is accompanied by a plastic deformation of particle volume and surface layers. By such a mechanism, it is possible to modify the surface structure (basal/edge ratio), the S/M composition and the catalytic activity of MoS_2 and WS_2 systems. The *in situ* prepared samples ATM-350 and ATT-350, which are deformated at intermediate uniaxial pressing, show the higher catalytic activity and surface areas. ATM-350 has the highest HDS selectivity of all the *in situ* catalysts.

5. Conclusions

The method of *in situ* activation of MoS_2 and WS_2 starting from ATM and ATT thiosalts yields catalysts with improved catalytic performance over *ex situ* catalysts. *In situ* catalysts show higher rates, improved stability to sintering and higher selectivity for hydrogenated products. Decomposition of thiosalts yields MoS_{2+x} *ex situ* and MoS_2C_x *in situ*; in the latter, carbon is found at the surface and is probably related to active sites.

Modification of the precursor thiosalts as a function of the mechanical pressure affects the properties of *in situ* MoS_2 and WS_2catalysts in the following ways:

(a) increases their surface area;

(b) changes their conversion activity, with the reaction rate going through a maximum at 350 MPa;

(c) decreases their surface S/M ratio, which is higher than stoichiometric for non-pressed samples and lower for samples pressed up to 700 MPa;

(d) changes their selectivity, with hydrogenation activity for MoS_2 going through a maximum at 350 MPa, and WS_2 showing only slight variation; cracking activity increases notably with pressure for WS_2 and remains the same for MoS_2.

Acknowledgement

The authors acknowledge funding for this research by the DGAPA-UNAM, through grant no. IN-102692. We thank Dr. M. Farías for fruitful discussion. We also thank E. Aparicio, I. Gradilla, G. Soto, J. Nieto and M. Sainz Romero for their valuable technical assistance. GA and MDV acknowledge fellowship support from CONACYT. The research stay of VP at CICESE is supported by DAIC-CONACYT through the "Cátedras Patrimoniales" program.

References

[1] G. Hagenbach, Ph. Courty and B. Delmon, J. Catal. 31 (1973) 264.
[2] R. Candia, B. Clausen and H. Topsøe, J. Catal. 77 (1982) 564.
[3] M. Zdrazil, Catal. Today 3 (1988) 269.
[4] O. Weisser and S. Landa, in: *Sulfide Catalysts: Their Properties and Applications* (Pergamon Press, Oxford, 1973).
[5] R. Frety, M. Breysse, M. Lacroix and M. Vrinat, Bull. Chem. Soc. Belg. 93 (1984) 663.
[6] K. Ramanathan and S. Weller, J. Catal. 95 (1985) 249.
[7] S. Fuentes, G. Diaz, F. Pedraza, H. Rojas and N. Rosas, J. Catal. 113 (1988) 535.
[8] K. Inamura and R. Prince, J. Catal. 147 (1994) 515.
[9] E. Frommell, J. Diehl, J. Tamilia and S. Pollack, in: Proc. 12th North American Meeting of the Catalytic Soc., Lexington, KY, 1991, PD-38.
[10] A. Naumann and A. Behan, US Patent 4,243,553 (1981).
[11] A. Naumann and A. Behan, US Patent 4,243,554 (1981).
[12] T. Pecoraro, R. Russell and R. Chianelli, US Patent 4,528,089 (1985).
[13] K. Brownlee, *Statistical Theory and Methodology in Science and Engineering*, 2nd Ed. (Wiley, New York, 1965) p. 590.
[14] H. Ishihara, T. Itoh, T. Hino, M. Nomura, P. Qi and T. Kabe, J. Catal. 140 (1993) 184.
[15] K. Liang, R. Chianelli, F.Z. Chien and S.C. Moss, J. Non-Cryst. Solids 79 (1986) 251.
[16] J. Brito, M. Ilija and P. Hernandez, Thermochim. Acta 256 (1995) 325.
[17] E. Rode and B. Lebedev, Zh. Neorg. Khim. 6 (1961) 1189.
[18] E. Diemann and A. Muller, Coord. Chem. Rew. 10 (1973) 79.
[19] R. Chianelli, Int. Rev. Phys. Chem. 2 (1982) 127.
[20] K. Pavlova, B. Panteleeva, E. Deryagina and I. Kalechits, Kinet. Katal. 6 (1965) 493.
[21] K. Voorhoeve and J. Stuiver, J. Catal. 23 (1971) 228.
[22] M. Del Valle, M. Yanez, M. Avalos and S. Fuentes, in: *Hydrotreating Technology for Pollution Control*, eds. M. Ocelli and R. Chianelli (1996) p. 47.
[23] H.W. Wang, P. Skeldon, G.E. Thompson and G.C. Wood, J. Mater. Sci. 32 (1997) 497.
[24] Y. Bensimon, P. Belougne, B. Deroide, J. Giuntini and J. Zanchetta. J. Phys. Chem. Solids 52 (1991) 471.
[25] P. Belougne, Y. Bensimon, B. Deroide, J. Giuntini and J. Zanchetta, Philos. Mag. B 67 (1993) 215.
[26] R. Fréty and M. Breysse, in: *Surface Properties and Catalysis by Non-Metals: Oxides, Sulfides and Other Transitional Metal Compounds*, eds. J. Bannelly, B. Delmon and E. Derouane (1993) p. 379.
[27] D. Kalthod and S. Weller, J. Catal. 95 (1985) 455.
[28] J. Bulicz, L. Morales de la Garza and S. Fuentes, Surf. Sci. 365 (1996) 411.
[29] P. Jensen, R. Frindt and S. Morrison, Mater. Res. Bull. 21 (1986) 457.
[30] C.N. Satterfield and T.K. Sherwood, *The Role of Diffusion in Catalysis* (Addison-Wesley, New York, 1963).
[31] V. Boldyrev, Solid State Ionics 63(5) (1993) 537.